

Case Report

Sporadic Creutzfeldt–Jakob disease with glial PrP^{Res} nuclear and perinuclear immunoreactivity

Ivan Fernández-Vega,^{1,2} Daniela Díaz-Lucena,^{3,4} Itxaso Azkune Calle,⁵ Maria Geijo,⁶ Ramon A. Juste,⁶ Franc Llorens,^{3,4} Ikerne Vicente Etxenautia,² Jorge Santos-Juanes,⁷ Juan Jose Zarranz Imirizaldu⁸ and Isidro Ferrer^{3,4,9,10} 

¹Pathology Department, Hospital Universitario Araba, ²Brain Bank Hospital Universitario Araba, Biobanco Vasco para la Investigación (O+eHun), Vitoria, ³Biomedical Research Institute of Bellvitge (IDIBELL), ⁴Biomedical Network Research Center of Neurodegenerative Diseases (CIBERNED), ⁵Department of Pathology and Experimental Therapeutics, University of Barcelona, ⁶Service of Pathologic Anatomy, Bellvitge University Hospital, Hospitalet de Llobregat, ⁷Neurology Department, Hospital Galdakao-Usansolo, Galdakao, ⁸Department of Animal Health, NEIKER-Tecnalia, Derio, ⁹Pathology Department, Hospital Universitario Central de Asturias, Oviedo and ¹⁰Neurology Department, Hospital Universitario de Cruces, Barakaldo, Spain

Proteinase K-resistant prion protein (PrP^{Res}) nuclear and perinuclear immunoreactivity in oligodendrocytes of the frontal cortex is found in one case of otherwise typical sporadic Creutzfeldt–Jakob disease (sCJD) type VV2a. The PrP nature of the inclusions is validated with several anti-PrP antibodies directed to amino acids 130–160 (12F10), 109–112 (3F4), 97–102 (8G8) and the octarepeat region (amino acids 59–89: SAF32). Cellular identification and subcellular localization were evaluated with double- and triple-labeling immunofluorescence and confocal microscopy using antibodies against PrP, glial markers, and histone H3. Based on review of the literature and our own experience, this is a very odd situation that deserves further validation in other cases.

Key words: astrocytes, Creutzfeldt–Jakob disease, oligodendrocytes, prion.

INTRODUCTION

Prion diseases are a group of transmissible encephalopathies linked to cellular prion protein (PrP^C) which is converted into an abnormally conformed proteinase K-resistant prion protein (PrP^{Res}). The human prion diseases are sporadic, iatrogenic or genetic Creutzfeldt–Jakob disease (sCJD, iCJD and gCJD, respectively), variant CJD, Gerstmann–Straüsler–Scheinker disease (GSS), and fatal

familial insomnia (FFI); gCJD, GSS, and FFI are due to mutations in the PPNP gene (*PPNP*)^{1–5}

sCJD is characterized clinically by rapid dementia accompanied by other neurological symptoms, and neuropathologically by neuronal loss, spongiform change, astrocytosis, microgliosis, and PrP^{Res} deposition.^{4,5} Several PrP types (types I and II, and variants) are recognized depending on the pattern of mono-glycosylated, di-glycosylated, and non-glycosylated prion.^{6,7} In addition, codon 129 (methionine or valine) in *PRNP* is largely contributory to clinical and neuropathological phenotypes.^{4,5} Moreover, PrP types correlate with characteristic PrP^{Res} deposits in tissue sections.⁸

PrP^{Res} deposits have particular patterns including diffuse/synaptic, patchy/perivacuolar, perineuronal, plaque-like, and kuru-like plaques, largely depending on the sCJD subtype.^{4,5,9} In addition, punctuate intracytoplasmic neuronal deposits, rows of PrP^{Res} deposits along myelinated fibers, and rare intracytoplasmic PrP^{Res}-positive granules in astrocytes and microglia are reported in CJD and other prionopathies.^{5,9–13}

The present report describes unique abundant intracytoplasmic PrP^{Res} nuclear and perinuclear immunoreactivity in astrocytes and oligodendrocytes in one case of sCJD VV2.

CASE PRESENTATION

A 66-year-old man had suffered from gait ataxia, cognitive impairment, sleeping difficulties, and myoclonus for the previous two months. There was no family history of neurological disease. Cerebrospinal fluid test was positive for 14-3-3 protein. EEG showed slow waves with periodic

Correspondence: Isidro Ferrer, MD, PhD, Department of Pathology and Experimental Therapeutics, University of Barcelona, c/Feixa Llarga sn, 08907 Hospitalet de Llobregat, Spain. Email: 8082ifa@gmail.com

Received 15 April 2018; Revised 15 June 2018; Accepted 05 July 2018.

synchronous discharges. Extensive cortical ribbon-like, basal ganglia, and cerebellum hyper-signals were noted on magnetic resonance imaging (MRI) examination. Progression of the disease was to a vegetative state. The patient died of bronchopneumonia four and a half months after clinical onset.

PATHOLOGICAL EXAMINATION

The brain weight was 1400 g. The left cerebral hemisphere was rapidly frozen and stored at -80°C for biochemical studies. Gross examination of the right cerebral hemisphere after 4% buffered formalin fixation revealed severe atrophy of the cerebellum, mainly involving the vermis, and the presence of a lacunar infarct in the internal capsule. Antemortem factors including agonal state, hypoxia, acidosis, fever, seizures, and medication were ruled out. Post-mortem factors were within normal limits. Post-mortem delay (interval between death and sample processing) was around 5 h and the duration of fixation was up to 3 weeks.

Microscopic examination revealed widespread microvacuoles (spongiform changes), mainly in the frontal and temporal cortex, with a laminar pattern involving the deep layers, hippocampus, striatum and thalamus, and the molecular layer of the cerebellum. Neuronal loss was found in all these regions and it was very marked in the cerebellum, affecting Purkinje cells and neurons of the granular layer; scattered axonal torpedoes were also observed in the granular layer. This was accompanied by marked astrogliosis and severe microglia. The cerebral white matter was normal. Neuronal loss and astrogliosis occurred in the mid-brain, and spongiform change was also observed in the pons. Immunohistochemistry with the 3F4 anti-PrP mouse monoclonal antibody (1:200; Millipore, Billerica, MA, USA) following proteinase K incubation (100 $\mu\text{g}/\text{mL}$; 37°C ; 1 h) and 10% formic acid for 1 h showed synaptic-like and frequent small granular plaque-like PrP^{Res} deposits, and perineuronal deposits in the neocortex and basal ganglia. Plaque-like PrP^{Res} deposits were abundant in the cerebellar cortex and white matter; synaptic-like PrP^{Res} immunoreactivity was present in the molecular layer as well. Small PrP^{Res}-immunoreactive dots (between 0.2 and 1.0 μm) were

present in the perikaryon of several neurons. In addition, PrP^{Res} nuclear (perinuclear) immunoreactivity was noted, apparently in the vicinity of, or within, glial nuclei in the frontal, parietal and temporal cortex. For PrP^{Res} identification of glial deposits, immunohistochemistry was performed using specific antibodies recognizing different PrP epitopes, conducted on 4- μm -thick paraffin sections following a protocol reported elsewhere.¹¹ To summarize, sections were first exposed to a combined pretreatment including hydrated autoclaving with 3 mM HCL acid (Merck, Kenilworth, NJ, USA) in distilled water incubated for 2 min after boiling, followed by 5 min incubation in 96% formic acid (Merck, Madrid, Spain) at room temperature. After washing, sections were incubated with serial proteinase K (PK) concentrations: 5, 10 and 20 $\mu\text{g}/\text{mL}$ for 15 min at 37°C , and were further blocked with Dako Real Peroxidase blocking solution (S2023, Dako, Barcelona, Spain). Sections were incubated overnight at 4°C with the primary antibodies, diluted in Dako Real Antibody Diluent (S2022, Dako) (Table 1). Afterwards, sections were incubated with MultiLink biotinylated antibody followed by horseradish peroxidase-conjugated streptavidin (QP9009L-E BioGenex detection kit, Fremont, CA, USA). Immunodetection was obtained after incubation with 3,3'-diaminobenzidine tetrahydrochloride (DAB) (D6737; Merck) and H_2O_2 . Sections were examined with a Nikon Eclipse E800 microscope with ProgRes[®] CapturePro 2.7.7 software (JENOPTIK, Jena, Germany). The results obtained using two additional anti-PrP antibodies, clones 12F10 and scrapie-associated fibril 32 (SAF32), were similar in the two assays (Fig. 1). Nuclear (perinuclear) immunoreactivity was not stained with anti-ubiquitin antibodies. No deposits of amyloid- β , hyperphosphorylated tau, α -synuclein, or transactivation response DNA-binding protein 43 kDa were observed.

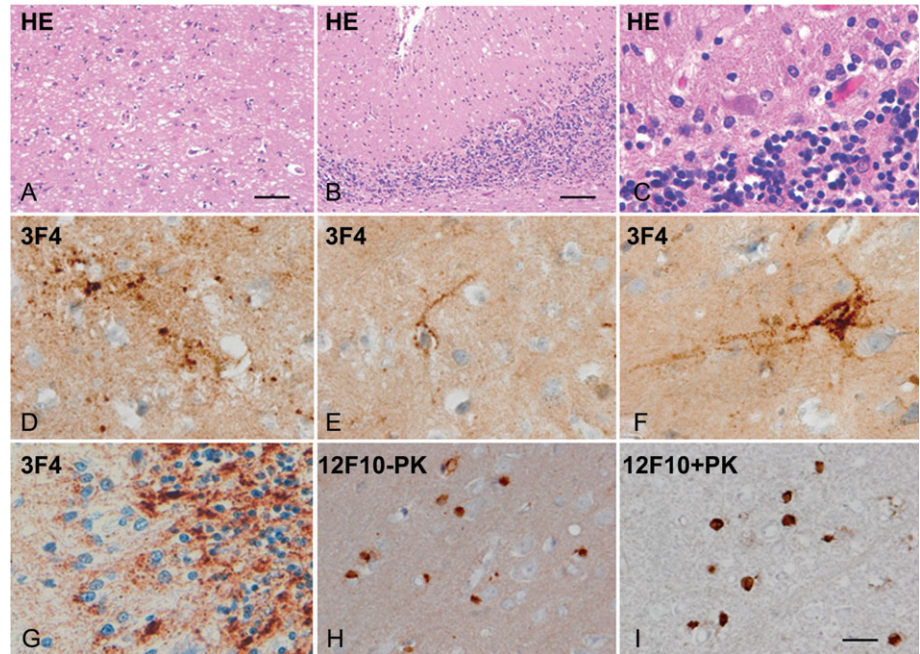
Genetic studies revealed no mutation in *PRNP* and valine homozygosity at codon 129. Western blotting with the antibody 3F4 (Dako) at a dilution of 1:3000 revealed a type II PrP^{Res} pattern; no bands of low molecular weight were present with this antibody.

In order to identify the characteristics and localization of PrP^{Sc} glial nuclear (perinuclear) immunoreactivity,

Table 1 Summary of antibodies used

Abbreviation	Name	Company	Ref. no.	Dilution	Target
12F10	Anti-PrP Clone 12F10	SPI-Bio	A03221	1:100	Region 130–160
3F4	Anti-PrP Clone 3F4	Millipore	MAB1562	1:100	Region 109–112
8G8	Anti-PrP Clone 8G8	SPI-Bio	A03220	1:50	Region 97–102
SAF32	Anti-PrP Clone SAF32	SPI-Bio	A03202	1:50	Region 59–89
Anti-GFAP	Anti-glial fibrillary acidic protein	Dako	Z0334	1:400	Astrocytes
Anti-H3	Anti-histone H3	Novus	NB100-747	1:50	Nuclei
Anti-Iba1	Anti-ionized calcium-binding adaptor molecule 1	Wako	019-19741	1:1000	Microglia
Anti-YKL40	Anti-chitinase-3-like protein 1 (CHI3L1)	Thermo-Fisher	PA5-43746	1:100	Astrocytes
Olig 2	Anti-oligodendrocyte transcription factor 2	Abcam	AB42453	1:500	Oligodendrocytes

Fig. 1 Histological (H&E; hematoxylin-eosin) (A-C) and immunohistochemical (D-I) observations of the brain. (A) Neuronal loss, spongiform change, and astrocytosis in the frontal cortex. (B) Spongiform change and loss of Purkinje cells in the cerebellum. (C) Spongiform change and astrocytosis in the Purkinje cell layer and inner molecular layer. (D) Synapse-like and granular proteinase K-resistant prion protein (PrP^{RES}) aggregates in the cerebral cortex. (E) Perineuronal positive immunostaining for PrP^{RES}. (F) Neuronal positive immunostaining for PrP^{RES}. (G) Neuronal positive immunostaining for PrP^{RES}. (H) Nuclear and perinuclear positive immunostaining for PrP^C in the frontal cortex. (I) Nuclear and perinuclear positive immunostaining for PrP^{RES} in the frontal cortex following proteinase K incubation for 20 min. Formalin-fixed, paraffin-embedded sections treated with formic acid. Scale bars: 40 μ m (A), 85 μ m (B), 25 μ m (C-I).



double- and triple-labeling immunofluorescence using specific neuronal and glial cell antibodies, and antibodies recognizing different PrP epitopes, was carried out in 4- μ m-thick de-waxed paraffin sections of the frontal cortex. Sections were first subjected to combined pretreatment¹¹ for PrP staining and then boiled in 10 mmol/L citrate buffer for 20 min. Sections were subsequently stained with a saturated solution of Sudan black B (Merck) for 15 min to block autofluorescence of lipofuscin granules, and then rinsed in 70% ethanol and washed in distilled water.

Afterwards, sections were blocked with 10% fetal bovine serum (FBS) for 1 h at room temperature, and incubated overnight at 4°C with appropriate diluted primary antibodies (Table 1). After washing, sections were incubated with Alexa-Fluor 488, 555, or 647 conjugated secondary antibodies (Molecular Probes, Eugene, OR, Life Technologies, Carlsbad, CA, Thermo Fisher Scientific Inc., Waltham, MA, USA, respectively). The sections were mounted in Immuno-Fluore mounting medium (ICN Biomedicals, Irvine, CA, USA), sealed, and dried overnight.

Fig. 2 Microphotographs by double-labeling immunofluorescence and confocal microscopy (A) and quantitative analysis of PrP antigens, microglial (α Iba1), astrocytic (α GFAP) and oligodendrocytic (Olig2) markers (B). (A) Nuclear and perinuclear areas of astrocytes (α GFAP) and oligodendrocytes (Olig2) are immunoreactive for PrP (3F4) and scrapie-associated PrP (SAF32). In contrast, there is no correlation between PrP (SAF32) and microglia (α Iba1). Formalin-fixed, paraffin-embedded sections. Scale bars: 20 μ m. (B) The percentage of PrP (SAF32)-immunoreactive cells colocalized in oligodendrocytes is significantly higher than in astrocytes and oligodendrocytes. Results are mean \pm SD of 2-3 sections. One-way analysis of variance shows significant difference ($P < 0.001$) of %SAF32 colocalized with the cell markers. Turkey's post hoc analysis reveals significant difference of %SAF32 with Olig2 with respect to %SAF32 colocalized with antibodies to Iba1 and GFAP (** $P < 0.001$).

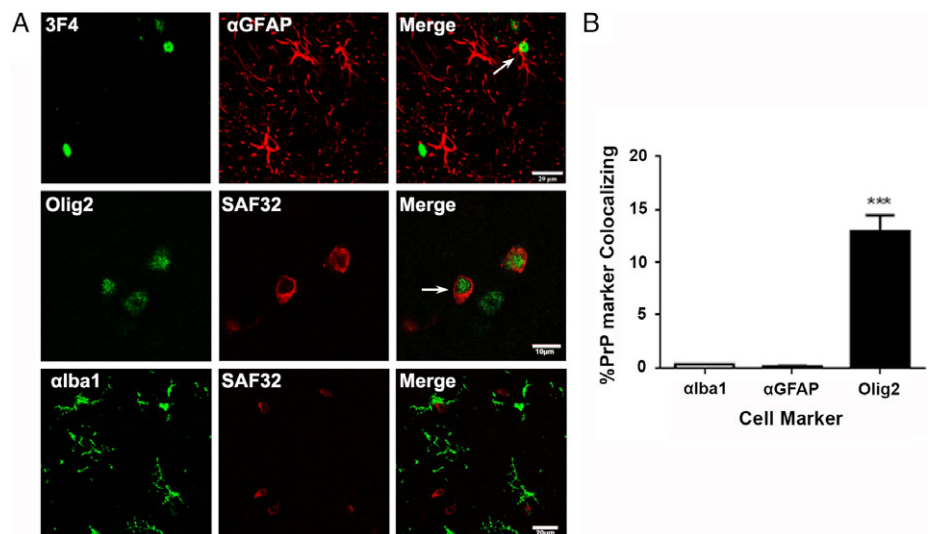


Table 2 Pearson's coefficient values for prion protein (PrP) and cell markers

Staining	PrP marker	Cell marker	Pearson's co-efficient
Double SAF32 + α Iba1	SAF32	α Iba1	0.001
Double SAF32 + α GFAP	SAF32	α GFAP	-0.031
Triple 12F10+ α H3 + α GFAP	12F10	α GFAP	0.023
Triple 12F10+ α H3 + α GFAP	12F10	α H3	0.084
Triple 12F10+ α H3 + α YKL40	12F10	α YKL40	0.261
Triple 12F10+ α H3 + α YKL40	12F10	α H3	0.215
Double SAF32 +Olig2	SAF32	Olig2	0.287
Triple 12F10+ α H3 +Olig2	12F10	Olig2	0.305
Triple 12F10+ α H3 +Olig2	12F10	α H3	0.240

Sections were examined with a Leica TCS-SL confocal microscope and analyzed for co-localization with Image J 1.8.0_112 using JACOP plugin (for Pearson's coefficient) and double-staining co-localization macros.

Double-labeling immunofluorescence to glial fibrillary acidic protein (GFAP) and PrP (3F4 antibody) showed significant PrP immunoreactivity in the vicinity of GFAP fibrils (Fig. 2A, upper row). Yet double-labeling with anti-oligodendrocyte transcription factor 2 antibody (Olig2) and SAF32 clearly showed PrP localization in the perinuclear region and within the nucleus of oligodendrocytes (Fig. 2A, middle row). No relationship was found between microglia identified with antibody to ionized calcium-binding adaptor molecule 1 (Iba1) and PrP deposits (Fig. 2A, lower row). Quantification of the percentage of cell markers with the PrP marker showed significant increase only in the %Olig2 that co-localized with %SAF32 (Fig. 2B). Moreover, Pearson's coefficient disclosed only a strong positive correlation between Olig2 and SAF32 (Table 2).

Similar PrP immunostaining was obtained with different anti-PrP antibodies directed to amino acids 130–160 (12F10), 109–112 (3F4), 97–102 (8G8), and the octarepeat region (amino acids 59–89: SAF32) as seen by double-labeling immunofluorescence to GFAP and PrP (Fig. 3).

Triple-labeling with distinct cellular markers, PrP antibodies, and anti-histone H3 revealed that most PrP immunoreactivity was localized within the nucleus or in the perinuclear region of oligodendrocytes, and rarely in astrocytes, including subpopulations of YKL40-immunoreactive astrocytes (Fig. 4). Pearson's coefficient showed a strong positive correlation of 12F10 with YKL40, Olig2, and cellular nuclei (Table 2).

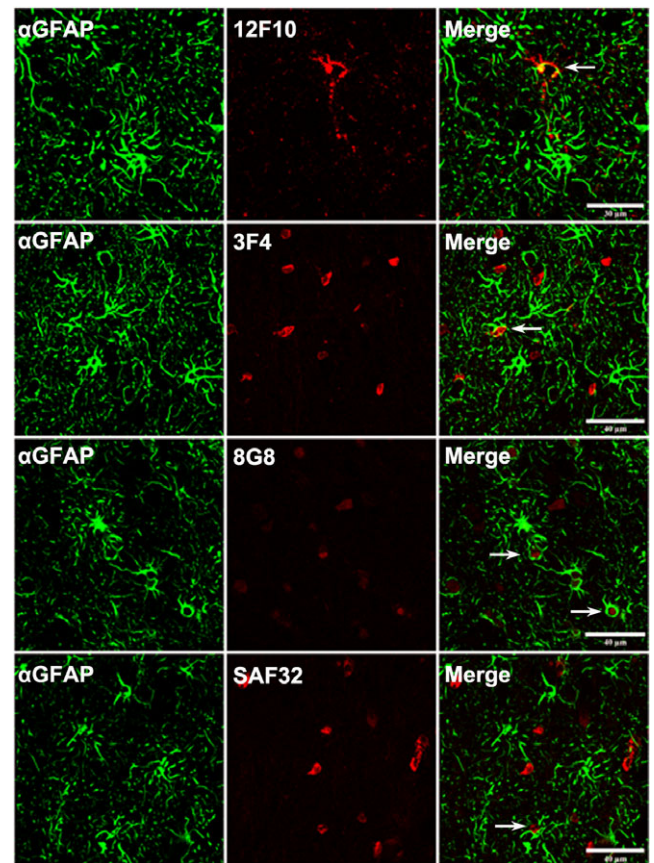


Fig. 3 Microphotographs by double-labeling immunofluorescence and confocal microscopy using antibodies to GFAP and different PrP antigens (12F10, 3F4, 8G8 and SAF32) showing a close relationship between nuclear and perinuclear immunoreactivity and astrocytes (arrows). Formalin-fixed, paraffin-embedded sections. Scale bars: 20 μ m (upper and lower rows), 10 μ m (middle rows).

DISCUSSION

Clinical symptoms, neuroimaging, genetics, neuropathological findings, and Western blot pattern of PrP^{Res} are typical of sCJD VV2a.^{4,5,8} Regarding PrP^{Res} deposition, synaptic-like and small granular plaque-like PrP^{Res} deposits, and perineuronal deposits in the neocortex and basal ganglia, together with plaque-like PrP^{Res} deposits in the cerebellar cortex and white matter, and synaptic-like PrP^{Res} immunoreactivity in the molecular layer in the present case, are consistent with sCJD VV2.⁵ In addition, punctate intraneuronal PrP immunoreactivity, here described as small PrP^{Res}-immunoreactive dots in the perikaryon, has been observed in scrapie, in experimental models of prion disease, and rarely, in sCJD.^{12–15}

Rare intra-cytoplasmic PrP^{Res} granules in human and animal prion diseases have been reported in microglia and astrocytes, suggesting that both cells may play a role in the processing, degradation and removal of PrP^{Res}.^{16,17} PrP^{Res} microsphere formation in the neuropil has been described in a rare case of familial CJD.¹⁸ However, nuclear and

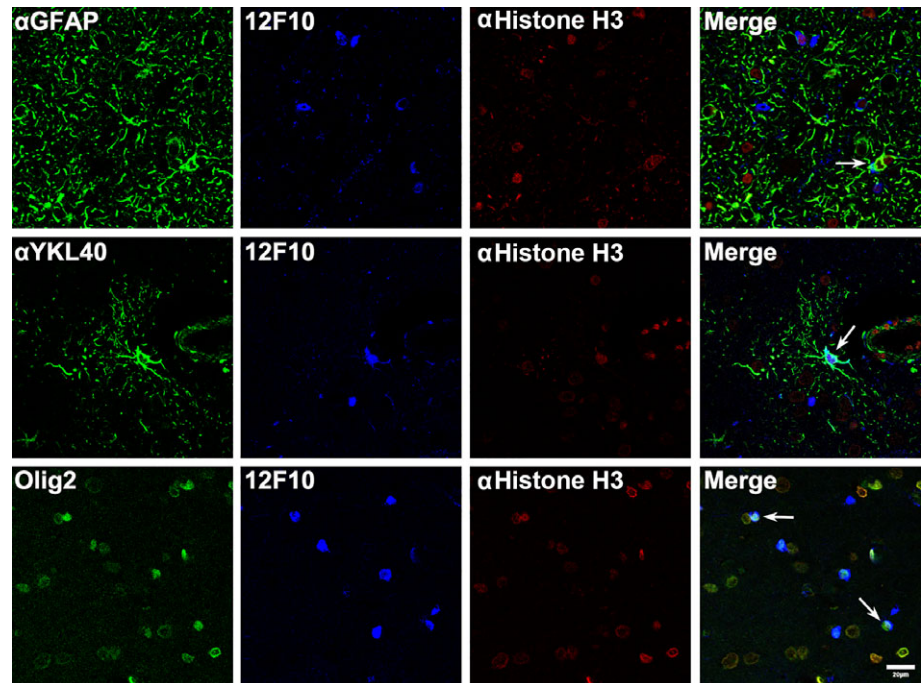


Fig. 4 Microphotographs by triple-labeling immunofluorescence and confocal microscopy using anti-GFAP, anti-YKL-40, Olig2, 12F10, and anti-histone H3. PrP immunoreactivity localizes in the nucleus of astrocytes and oligodendrocytes (arrows). Formalin-fixed, paraffin-embedded sections. Scale bars: 20 μ m.

perinuclear immunoreactivity in cortical astrocytes and oligodendrocytes as observed here have not been previously reported to our knowledge.

The PrP nature of these deposits is supported by the recognition of similar staining using different anti-PrP antibodies directed against different epitopes of the prion protein, including 12F10 (amino acids 130–160), 3F4 (amino acids 109–112), 8G8 (amino acids 97–102), and SAF32 (amino acids 59–89).

PrP immunoreactivity in the inclusions is mostly PK-resistant; PrP immunoreactivity is maintained at PK concentrations of 20 μ g/mL. Double- and triple-labeling of PrP with different neuronal and glial cell markers, and histone H3, clearly demonstrates the glial localization of PrP immunoreactivity mainly in the nucleus and perinuclear region in oligodendrocytes.

PrP^C is normally expressed in neurons, astrocytes, and oligodendrocytes during development and adulthood.¹⁹ Functions of PrP^C during development include modulation of the differentiation of human stem cells into neurons, astrocytes, and oligodendrocytes.^{20,21} Therefore, the PrP deposits here observed in glial cells are probably produced in the same cells. How the conversion of PrP^C into PrP^{Res} is produced in oligodendrocytes is not known, as oligodendrocytes are apparently resistant to PrP^{Res} infectivity.²²

The nuclear localization of glial PrP immunoreactivity is curious. However, nuclear localization of normal and abnormal PrP has been reported in various settings. Abnormal transport of C-terminally truncated and abnormally glycosylated mutant PrP to the nucleus has been reported in cell models of familial prion disorders associated with a stop

codon mutation at residues 145 or 160 of the PrP.²³ The N-terminal region of human and ovine PrP has been described as harboring nucleic acid binding and chaperoning properties.²⁴ When acting together, two independent nuclear localization signals in the N-terminal domain of PrP complement each other in transporting the N-terminal fragment of PrP to the nucleus of transfected cells, where it accumulates.²⁵

In addition to truncated forms, PrP^C can localize in the nucleus of different cell types including neural cells, and it interacts with structural chromatin components, principally histone H3; the interaction of PrP^C with histone H3 suggests that PrP is involved in transcriptional regulation in the nucleus.^{26,27} Nuclear PrP interacts with distinct proteins involved in cell proliferation and cell junction in several cell types,²⁸ and PrP participates in the process of DNA repair after genotoxic stress.²⁹

It may be argued that the PrP immunostaining here observed is not simply up-regulation of PrP for any reason. However, we have spent many years studying hundreds of brains with CJD using similar methodological procedures and the same routine protocols, and have never before observed those intriguing inclusions. The present findings in a single case must be corroborated in additional cases to prove that, although rarely, PrP^{Res} can be localized in the cytoplasm and nucleus of glial cells, mainly oligodendrocytes, in CJD.

ACKNOWLEDGMENTS

We thank the Basque Biobank for Research-OEHUN for its collaboration. We wish to thank T. Yohannan for editorial assistance.

DISCLOSURE

The authors declare no conflicts of interest for this article.

REFERENCES

- Prusiner SB. An introduction to prion biology and diseases. In: Prusiner SB, (ed). *Prion Biology and Diseases*, 2nd edn. New York: Cold Spring Harbor Laboratory, 2004; 1–87.
- Aguzzi A. Prion diseases of humans and farm animals: Epidemiology, genetics, and pathogenesis. *J Neurochem* 2006; **97**: 1726–1739.
- Gambetti P, Cali I, Notari S, Kong Q, Zou WQ, Surewicz WK. Molecular biology and pathology of prion strains in sporadic human prion diseases. *Acta Neuropathol* 2011; **121**: 79–90.
- Budka H, Head MW, Ironside JW, Gambetti P, Parchi P, Tagliavini F. Sporadic Creutzfeldt-Jakob disease. In: Dickson DW, Weller RO, (eds). *Neurodegeneration: The Molecular Pathology of Dementia and Movement Disorders*, 2nd edn. Chichester: Wiley-Blackwell, 2011; 322–335.
- Head MW, Ironside JW, Ghetti B, Jeffrey M, Piccardo P, Will RG. Prion diseases. In: Love S, Budka H, Ironside JW, Perry A, (eds). *Greenfield's Neuropathology*, 9th edn. Boca Raton, FL: CRC Press, Taylor & Francis Group, 2015; 1016–1086.
- Parchi P, Giese A, Capellari S *et al.* Classification of sporadic Creutzfeldt-Jakob disease based on molecular and phenotypic analysis of 300 subjects. *Ann Neurol* 1999; **46**: 224–233.
- Parchi P, Notari S, Weber P *et al.* Inter-laboratory assessment of PrPSc typing in Creutzfeldt-Jakob disease: A western blot study within the NeuroPrion Consortium. *Brain Pathol* 2009; **19**: 384–391.
- Parchi P, de Boni L, Saverioni D *et al.* Consensus classification of human prion disease histotypes allows reliable identification of molecular subtypes: An inter-rater study among surveillance centres in Europe and USA. *Acta Neuropathol* 2012; **124**: 517–529.
- Kovacs GG, Head MW, Hegyi I *et al.* Immunohistochemistry for the prion protein: Comparison of different monoclonal antibodies in human prion disease subtypes. *Brain Pathol* 2002; **12**: 1–11.
- El Hachimi KH, Chaunu MP, Brown P, Foncin JF. Modifications of oligodendroglial cells in spongiform encephalopathies. *Exp Neurol* 1998; **154**: 23–30.
- Kordek R, Hainfellner JA, Liberski PP, Budka H. Deposition of the prion protein (PrP) during the evolution of experimental Creutzfeldt-Jakob disease. *Acta Neuropathol* 1999; **98**: 597–602.
- Kovacs GG, Head MW, Bunn T, Laszlo L, Will RG, Ironside JW. Clinicopathological phenotype of codon 129 valine homozygote sporadic Creutzfeldt-Jakob disease. *Neuropathol Appl Neurobiol* 2000; **26**: 463–472.
- Gonzalez L, Martin S, Jeffrey M. Distinct profiles of PrP(d) immunoreactivity in the brain of scrapie- and BSE-infected sheep: Implications for differential cell targeting and PrP processing. *J Gen Virol* 2003; **84**: 1339–1350.
- Jeffrey M, McGovern G, Siso S, Gonzalez L. Cellular and sub-cellular pathology of animal prion diseases: Relationship between morphological changes, accumulation of abnormal prion protein and clinical disease. *Acta Neuropathol* 2011; **121**: 113–134.
- Kovacs GG, Molnar K, Keller E, Botond G, Budka H, Laszlo L. Intraneuronal immunoreactivity for the prion protein distinguishes a subset of E200K genetic from sporadic Creutzfeldt-Jakob disease. *J Neuropathol Exp Neurol* 2012; **71**: 223–232.
- Jeffrey M, Goodsir CM, Bruce ME, McBride PA, Farquhar C. Morphogenesis of amyloid plaques in 87V murine scrapie. *Neuropathol Appl Neurobiol* 1994; **20**: 535–542.
- Kovacs GG, Preusser M, Strohschneider M, Budka H. Subcellular localization of disease-associated prion protein in the human brain. *Am J Pathol* 2005; **166**: 287–294.
- Honda H, Ishii R, Hamano A *et al.* Microsphere formation in a subtype of Creutzfeldt-Jakob disease with a V180I mutation and codon 129 MM polymorphism. *Neuropathol Appl Neurobiol* 2013; **39**: 844–848.
- Moser M, Colello RJ, Pott U, Oesch B. Developmental expression of the prion protein gene in glial cells. *Neuron* 1995; **14**: 509–517.
- Bribián A, Fontana X, Llorens F *et al.* Role of the cellular prion protein in oligodendrocyte precursor cell proliferation and differentiation in the developing and adult mouse CNS. *PLoS One* 2012; **7**: e33872.
- Leey YJ, Baskakov IV. The cellular form of the prion protein guides the differentiation of human embryonic stem cells into neuron-, oligodendrocyte-, and astrocyte-committed lineages. *Prion* 2014; **8**: 266–275.
- Prinz M, Montrasio F, Furukawa H *et al.* Intrinsic resistance of oligodendrocytes to prion infection. *J Neurosci* 2004; **24**: 5974–5981.
- Lorenz H, Windl O, Kretzschmar HA. Cellular phenotyping of secretory and nuclear prion proteins associated with inherited prion diseases. *J Biol Chem* 2002; **277**: 8508–8516.
- Gabus C, Derrington E, Leblanc P *et al.* The prion protein has RNA binding and chaperoning properties characteristic of nucleocapsid protein NCP7 of HIV-1. *J Biol Chem* 2001; **276**: 19301–19309.
- Gu Y, Hinnerwisch J, Fredricks R, Kalepu S, Mishra RS, Singh N. Identification of cryptic nuclear

- localization signals in the prion protein. *Neurobiol Dis* 2003; **12**: 133–149.
26. Strom A, Wang GS, Picketts DJ, Reimer R, Stuke AW, Scott FW. Cellular prion protein localizes to the nucleus of endocrine and neuronal cells and interacts with structural chromatin components. *Eur J Cell Biol* 2011; **90**: 414–419.
 27. Cai H, Xie Y, Hu L, Fan J, Li R. Prion protein (PrP (c)) interacts with histone H3 confirmed by affinity chromatography. *J Chromatogr B Analyt Technol Biomed Life Sci* 2013; **929**: 40–44.
 28. Rousset M, Leturque A, Thenet S. The nucleojunctional interplay of the cellular prion protein: A new partner in cancer-related signaling pathways? *Prion* 2016; **10**: 143–152.
 29. Bravard A, Auvré F, Fantini D *et al.* The prion protein is critical for DNA repair and cell survival after genotoxic stress. *Nucleic Acids Res* 2015; **43**: 904–916.